Quenching Mechanism of Rose Bengal Triplet State Involved in Photosensitization of Oxygen in Ethylene Glycol

Okiyasu Shimizu,*,† Jun Watanabe,† Shizuo Naito,‡ and Yasushi Shibata†

Photobiophysics Laboratories, Graduate School of Natural Sciences, Nagoya City University, Mizuho-ku, Nagoya 467-8501, Japan, and Faculty of Economics and Information, Gifu Shotoku Gakuen University, Gifu 500-8288, Japan

Received: October 24, 2005; In Final Form: December 10, 2005

The quenching rate constants of the excited triplet state of Rose Bengal (RB) by oxygen (k_{obs}) were measured in ethylene glycol (EG) at different temperatures using nanosecond laser flash photolysis. Although a plot of the quenching rate constant k_{obs} for RB triplet state vs oxygen concentration is linear at 20 °C, the oxygen dependence of k_{obs} does not exhibit linearity but upward curvature at high temperatures from 130 to 140 °C. The upward curvature at high temperatures is not well-described by a kinetic scheme first postulated by Gijzeman et al., which is characterized by exciplex formation and a unimolecular dissociation of the exciplex to products, but instead by a more comprehensive mechanism involving a bimolecular dissociation in addition to a unimolecular one. The measurements of the oxygen dependence of k_{obs} for RB triplet state at different temperatures yielded a reaction enthalpy for the exciplex formation of 150 kJ mol^{-1}. Due to the large exothermic reaction enthalpy, equilibrium was obtained for the exciplex at 20 °C even at low oxygen concentration and the bimolecular quenching by oxygen became the major dissociation process. The equilibrium attainment and bimolecular dissociation provide a linear oxygen dependence of k_{obs} to all outward appearances. Therefore, linearity does not always mean that exciplex dissociation proceeds solely through a unimolecular mechanism.

Introduction

The lowest excited state $^1\Delta_g$ of molecular oxygen, singlet oxygen, $O_2(^1\Delta_g)$, is extremely reactive and highly cytotoxic, and it is responsible for the breakdown of cellular microstructures and cell death;[1−3] it also has significant applications in a variety of areas, including organic synthesis[4,5] and photodynamic cancer therapy.[6,7] Experimental and theoretical research resulting in both the formation and the removal of $O_2(^1\Delta_g)$ in solution systems has been carried out extensively over the past four decades.[8−27] Singlet oxygen can be readily and efficiently produced through photosensitization of oxygen. Since singlet states of oxygen lie below the triplet-state energy of most organic molecules used as sensitizers,[28] oxygen quenches the triplet states of sensitizers added or inherent to a system by both enhancement of intersystem crossing and intermolecular energy transfer of excitation to ground-state oxygen.

Since the work of Gijzeman et al.,[10,11] the oxygen quenching of the excited triplet-state sensitizer, $^3S^*$, has been believed to proceed through the formation of exciplex, $(S\cdots O_2)^*$, and unimolecular dissociation to give products such as $O_2(^1\Delta_g)$, oxygen, and a ground-state sensitizer, as shown in Scheme 1. The overall process may be governed by spin statistics to provide an efficiency of $O_2(^1\Delta_g)$ produced during oxygen quenching of $^3S^*$. Scheme 1 has been the basis for a large number of studies carried out over the past 30 years regarding photosensitization and $O_2(^1\Delta_g)$ formation.[29−46] In fact, however, exciplex formation rates lack for a spin statistical effect,[34] and the quantum yield of $O_2(^1\Delta_g)$ varies significantly depending on various parameters, including the physical properties of the sensitizer,[10] the solvent environment,[31] and so on. In Scheme 1, a plot of the quenching rate constant vs oxygen concentration is characterized by a right rectangular hyperbola and shows linearity at low oxygen concentrations, approaching a slope of zero at the limit of infinite concentration.[19] As such, the linearity alone does not necessarily substantiate the validity of Scheme 1 for the oxygen quenching of $^3S^*$, as no curvature can be observed at high O_2 concentrations. The data published hitherto have showed linearity but have demonstrated no curvature at high O_2 concentrations soluble in solution.[19,20]

SCHEME 1

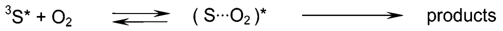

In studying the kinetic process involving the oxygen exciplex, experiments at high temperatures are effective for obtaining a transient phenomenon closely related to the exciplex dissociation forming reactants. Ethylene glycol is available as a solvent for experiments carried out in solution at high temperatures because it exists in a liquid phase up to 197 °C at 1 atm. Rose Bengal (RB) has been used extensively as a photosensitizer for inactivating biological molecules and cells via the production of $O_2(^1\Delta_g)$.[47,48] The photophysical and photochemical properties of heavy atom-substituted xanthene dyes such as RB are notable for their high triplet quantum yields of approximate unity and for triplet states with fairly long lifetimes from 0.1 to 0.3 ms.[49] Triplet−triplet (T−T) absorption bands have been reported to be observed in the near-IR region around 1000 nm by laser flash photolysis, which allows for precise measurements without disturbance by both luminescence and strong absorption bands of dyes in the visible region.[50]

In the present study, we observed the transient T−T absorption spectra of RB in ethylene glycol by laser flash photolysis

---

* To whom correspondence should be addressed. E-mail: shimizu@nsc.nagoya-cu.ac.jp. Tel: +81-52 (872) 5844. Fax: +81-52 (872) 5847.

† Nagoya City University.

‡ Gifu Shotoku Gakuen University.

10.1021/jp056073s CCC: $33.50

and obtained a nonlinear dependence of the quenching rate constant on oxygen concentration at high temperatures from 130 to 140 °C. The nonlinearity at low O_2 concentrations indicates that a comprehensive mechanism including Scheme 1 is required for the quenching process of excited triplet states of sensitizers by oxygen. We expect that our results will stimulate further investigations not only of the generation efficiency of $O_2(^1\Delta_g)$ but also in various fields related to photosensitization.

Material and Methods

RB and spectrophotometric ethylene glycol (EG) were obtained from Sigma-Aldrich Co., Ltd. A low concentration (5.0 × 10^{-6} M (1 M = 1 mol·L $^{-1}$)) of RB was used to minimize the aggregation in EG,[51] and the absorbance was measured to be 0.15 at 532 nm using a Shimadzu UV240 spectrophotometer. All measurements were performed on a near-IR-sensitive flash photolysis apparatus built in our laboratory.[52] The flash photolysis was carried out using 532-nm output from a Nd:YAG laser (New Wave Research, Tempest-10, 5 ns full width at half maximum) with a pulse energy of 0.31 mJ. The monitoring light perpendicular to the exciting pulse was obtained from a 150 W xenon arc lamp with a cutoff filter (Toshiba R-69) transmitting $\lambda > 690$ nm. The pulse energy at 532 nm was measured using a pyroelectric radiometer from Ophir Optronics equipped with a detector head PE25. To detect the monitoring light after it passed through a sample cell and a monochromator, a Hamamatsu G3476-05 InGaSi-PIN photodiode was employed in the near-IR wavelength region. The signals were recorded on a Tektronics TDS3052 digital oscilloscope with the highest time resolution of 0.2 ns and were averaged from 16 to 256 laser shots to improve the signal-to-noise ratio.

For the laser flash photolysis, to minimize the photodegradation of the sensitizer (RB), the sample solution introduced from a cylinder containing fresh sample was made to flow through a 3 mm × 10 mm × 50 mm flow cell into another cylinder of waste sample at a rate appropriate for measurements by a tubing pump. Both the cylinder of fresh sample and the cell holder were freely kept at a constant temperature ranging from 10 to 150 °C by circulating water or poly(ethylene glycol) around them. The temperature was measured by a thermocouple placed just above the light path in the flow cell. The oxygen concentrations in both cylinders were controlled by bubbling the solutions for 30 min before and during the measurement at a constant temperature with an equilibrium mixture of a known ratio of nitrogen and oxygen gas, which was obtained by using calibrated Kofloc gas-flow meters (Kyoto, Japan).

Oxygen concentrations were calculated using Henry's law, assuming a concentration of 5.8 × 10^{-4} M in oxygen-saturated EG at 1 atm and 20 °C.[28] Further, O_2 concentrations in EG at high temperatures from 130 to 140 °C were also obtained by flash photolysis using a quartz cuvette equipped with a tiny balloon of silicon rubber to keep the inside at atmospheric pressure in any temperature range. After the RB solution of EG at high temperature was sealed in the cuvette, we measured the rate constant of T−T absorption decay of RB in the cuvette at 20 °C and atmospheric pressure. When a calibration curve of O_2 concentration vs the rate constant of RB T−T absorption decay at 20 °C was used, O_2 concentrations of 5.2 × 10^{-4}, 5.1 × 10^{-4}, 4.7 × 10^{-4}, 4.5 × 10^{-4}, and 4.2 × 10^{-4} M were obtained in O_2-saturated EG at 1 atm and 130, 132, 135, 137, and 140 °C, respectively, after corrections for volume expansion of EG due to increasing temperature.

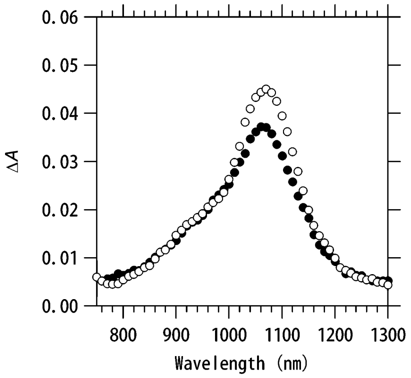

Figure 1. Transient absorption spectra after 532-nm laser pulsing of 5-μM Rose Bengal in N_2-saturated ethylene glycol at 20 °C (○) and 140 °C (●).

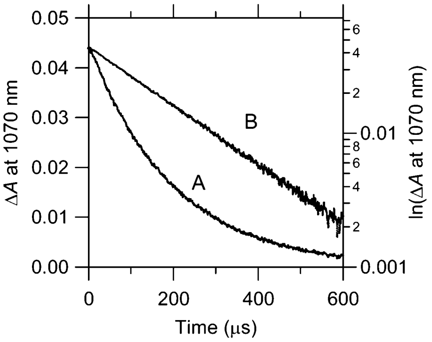

Figure 2. Decay of the transient T−T absorption of RB at 1070 nm in the 532-nm laser-photolyzed N_2-saturated EG solution at 20 °C (A) with absorbance in the logarithmic scale vs time (B).

Results and Discussion

Transient absorption spectra in the range of 750 to 1300 nm were obtained from the plot of initial values of decay after 532-nm laser photolysis of RB in ethylene glycol. Since the optical absorption by ground-state molecules of RB is negligible in the near-IR region, the measured absorbance was equal to the absorbance due to only the excited-state species in the near-IR region. The transient absorption spectra were observed by the 532-nm laser photolysis of RB in N_2-saturated EG at 20 and 140 °C, as shown by the open and solid circles in Figure 1, respectively. Although the absorption at 140 °C is somewhat smaller than that at 20 °C, both spectra with peaks around 1070 nm can be attributed to the triplet−triplet (T−T) transient absorption band due to the T−T transition of RB based on their similarity to the reported T−T absorption of other xanthene dyes.[53]

Figure 2 shows the decay of the transient T−T absorption of RB at 1070 nm in the 532-nm laser-photolyzed N_2-saturated EG solution at 20 °C (A) with the absorbance in logarithmic scale vs time (B).

The logarithmic profile of the T−T absorption band of RB is linear, and the decay is single exponential with a rate constant of 5.12 × 10^3 s^{-1} at 20 °C in N_2-saturated ethylene glycol. Since the observation of the rapid T−T absorption depends on the presence of an adequate concentration of the absorbing triplet species, the T−T absorption decay of RB reflects the concentration change of the first excited triplet state of RB in solution.

The excited triplet states of RB were effectively quenched by O_2 in the photolyzed EG solution at 20 °C, as shown in Figure 3 as a typical instance. Figure 3 indicates the decay of the T−T absorption of RB for the 70% O_2-saturated EG solution (A) and the ratio to the N_2-saturated solution (B) at 20 °C in

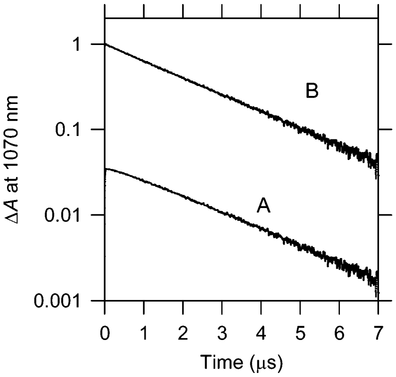

Figure 3. Decay of the T−T absorption of RB for the 532-nm laser-photolyzed solution of 70% O_2-saturated EG (A) and the ratio to N_2-saturated EG (B) at 20 °C in the logarithmic scale.

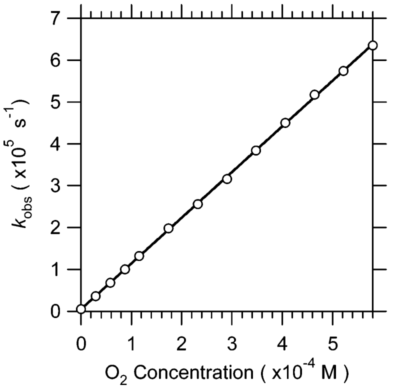

Figure 4. Plots of the rate constant k_{obs} as a function of O_2 concentration in the 532-nm laser-photolyzed RB solution of ethylene glycol at 20 °C. A straight line fitted to the data points was used as an experimental equation for a calibration to obtain the O_2 concentration in EG at high temperatures, as mentioned in the text.

logarithmic scale. Although the T−T absorption decay in logarithmic scale (A) clearly shows a slight deviation from linearity due to the decay characteristic of RB as shown by the initial stage of the curve (A) in Figure 2, the logarithmic ratio to the N_2-saturated solution vs time gives a straight line (B) and a quenching attributed to O_2 is characterized by a single-exponential decay with a rate constant of 4.45×10^5 s^{-1}. Therefore, the quenching rate constant k_{obs} of the RB triplet states by O_2 in the 70% O_2-saturated EG solution was evaluated to be the sum of the rate constants for the ratio and the 532-nm laser-photolyzed N_2-saturated EG solution at 20 °C, that is, 4.50×10^5 s^{-1}. Plots of the rate constant k_{obs} determined in this way are shown in Figure 4 as a function of the O_2 concentration in the 532-nm laser-photolyzed RB solution of EG at 20 °C. The linear dependence of the rate constant k_{obs} on O_2 concentration is in agreement with the reported features of the quenching rate constant concerning photosensitization at room temperature.[19,20] A straight line fitted to data points in Figure 4, which was used as an experimental equation for a calibration to obtain the O_2 concentration in EG at high temperatures as mentioned above, is expressed by eq 1

$$k_{obs} = 5.09 \times 10^{3} + 1.09 \times 10^{9}\,[O_2] \qquad (1)$$

where k_{obs} and $[O_2]$ are in units of s^{-1} and mol·L^{-1}, respectively.

Figure 5 shows the plots of temperature dependence of k_{obs} vs oxygen concentration in the 532-nm laser-photolyzed RB solution of EG at 130 (A), 132 (B), 135 (C), 137 (D), and 140 °C (E) together with data at 20 °C (F). The slopes increase with increasing temperature over a range from 20 to 140 °C. However, each plot of k_{obs} loses linearity at low O_2 concentrations with increasing temperature above 130 °C. For the purpose of clarity, a plot of k_{obs} as a function of O_2 concentration at 140 °C is denoted in Figure 6. There are a few noticeable features regarding the plot in this figure. The value of the quenching constant k_{obs} of the excited triplet states of RB at 140 °C increases, depicting an upward curvature with increasing O_2 concentration and asymptotically rises up toward a straight line with a slope. It is characteristic of the straight line part that its extrapolate does not go through the origin but intercepts the abscissa. The upward curvature is a clear indication that the triplet-state quenching of RB does not proceed through a simple elementary reaction but a kind of balanced state involving O_2. Further, the asymptote with a slope suggests attainment of a stationary concentration of the intermediate state, together with the presence of another triplet-state quenching involving additional O_2 to give products.

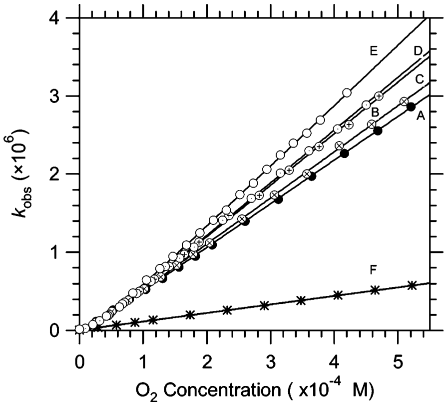

Figure 5. Plots of the temperature dependence of k_{obs} vs oxygen concentration in the 532-nm laser-photolyzed RB solution of ethylene glycol at 130 (A), 132 (B), 135 (C), 137 (D), and 140 °C (E) together with data at 20 °C (F).

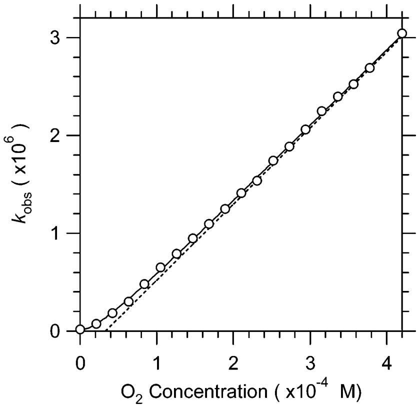

Figure 6. Plot of k_{obs} vs O_2 concentration in the 532-nm laser-photolyzed RB solution of ethylene glycol at 140 °C. The solid line indicates the fitting curve obtained by applying eq 3 to the experimental data points for k_{obs}. The dotted line shows an asymptote calculated from kinetic parameters obtained at 140 °C.

To explain the dependence of k_{obs} on the O_2 concentration in the RB solution of EG, Scheme 2 is introduced on the basis of the above speculations. On the basis of this scheme, one can obtain eq 2

$$\frac{d}{dt}([^3S^*] + [(S\cdots O_2)^*]) = -k_0[^3S^*] - k_p[(S\cdots O_2)^*] - k_d[(S\cdots O_2)^*][O_2] \qquad (2)$$

SCHEME 2

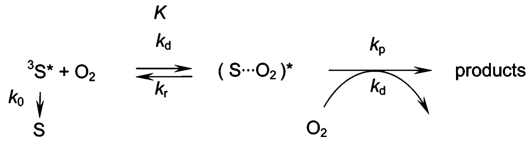

TABLE 1: Kinetic Parameters Related to the Quenching Rate Constant k_{obs} at Different Temperatures

temperature (°C)	k_0 (s^{-1})	k_p (s^{-1})	k_d (M^{-1} s^{-1})	K (M^{-1})
130	1.10×10^4	5.39×10^3	5.59×10^9	8.75×10^4
132	1.15×10^4	5.10×10^3	5.91×10^9	6.70×10^4
135	1.24×10^4	4.16×10^3	6.62×10^9	4.59×10^4
137	1.31×10^4	4.22×10^3	6.77×10^9	4.21×10^4
140	1.41×10^4	4.92×10^3	7.78×10^9	2.96×10^4

where square brackets denote the concentrations, k_0 is the unimolecular rate constant of radiative and radiationless transitions of the triplet sensitizer to the ground-state molecule S, K is the equilibrium constant for the exciplex formation, k_p is the unimolecular rate constant of the exciplex dissociation leading to products, and k_d is the bimolecular rate constant for the exciplex breakdown to products through the interaction with O_2. Assuming a rapid and reversible formation of the exciplex between triplet sensitizer, $^3S^*$, and O_2, the rate constant for the overall quenching process, k_{obs}, is given by

$$k_{obs} = \frac{k_0 + k_pK[O_2] + k_dK[O_2]^2}{1 + K[O_2]} \qquad (3)$$

The solid line in Figure 6 indicates the fitting curve obtained by applying the eq 3 to the experimental data points for k_{obs}. A dotted line shows an asymptote calculated from kinetic parameters obtained at 140 °C. The best fit between the theoretical function and data points proves that the quenching mechanism of triplet-state RB by O_2 is well-described by Scheme 2. If the quenching of $^3S^*$ by O_2 occurs only via a unimolecular dissociation from the exciplex, it should be noted that the rate constant may approach a constant value with an increase in O_2 concentration. In our case, however, the quenching takes place linearly without reaching a constant value with increasing O_2 concentrations. Thus, $(S\cdots O_2\ )^*$ dissociates with the bimolecular rate constant k_d of 7.78×10^9 M^{-1} s^{-1} in addition to the unimolecular rate constant k_p of 4.92×10^3 s^{-1} at 140 °C. Moreover, the unimolecular rate constant for the exciplex breakup forming reactants, k_r, of 2.63×10^5 s^{-1} can be derived from $k_r = k_d/K$ using k_d, of 7.78×10^9 M^{-1} s^{-1}. Therefore, we obtain the occurrence probability of 0.02 ($= k_p/(k_p + k_r)$) for the unimolecular dissociation paths of $(S\cdots O_2)^*$ at 140 °C.

The best-fit values of k_0, k_p, k_d, and K are given in Table 1 at different temperatures. The kinetic functions for each temperature are shown as solid lines fitted to data in Figure 5. Although the unimolecular rate constant k_p is little affected by temperature, the equilibrium constant for the exciplex formation, K, increases approximately three times higher by a slight decrease in temperature from 140 to 130 °C. $R \ln K$ plotted against $1/T$ is given in Figure 7, where R denotes the gas constant. The plot is reasonably straight, and the solid line in the figure is the fitting line expressed in units of J K^{-1} mol^{-1} by eq 4

$$R \ln K = -2.68 \times 10^{2} + 1.46 \times 10^5/T \qquad (4)$$

The slope is 1.46×10^5, so the reaction enthalpy of the exciplex formation is estimated to be ca. 150 kJ mol^{-1}, which is quite a bit larger than the activation energy of 45 kJ mol^{-1} obtained for the decomposition of the exciplex between oxygen and the triplet state of methylbenzanthracene in 3-methylpentane, though the argument was based on Scheme 1.[39] The equilibrium constant estimated by eq 4 is 1.11×10^{12} for the exciplex formation at 20 °C. This means that even at the minimum oxygen concentration of 2.9×10^{-5} M in our experiment, almost all excited species may be in the exciplex state $(S\cdots O_2\ )^*$ at 20 °C and that the quenching occurs predominantly through the bimolecular process. Actually, when eq 3 was applied to the experimental data points for k_{obs} at 20 °C, values of 5.08×10^3 s^{-1} and 1.11×10^{12} M^{-1} s^{-1} were obtained for k_p and K, respectively, together with k_d of 1.09×10^9 s^{-1}, and the corresponding asymptote was expressed by $k_{obs}{}^{asymptte} = 5.08 \times 10^3 + 1.09 \times 10^9\ [O_2\ ]$ in agreement with experimental eq 1.

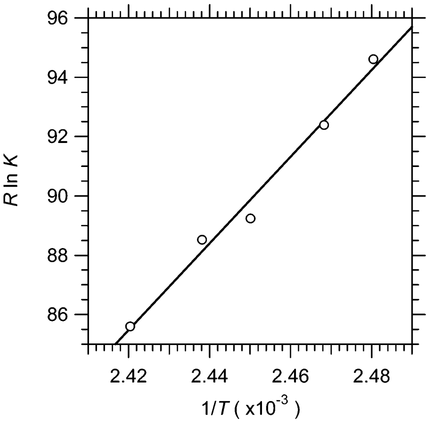

Figure 7. Plot of $R \ln K$ against $1/T$ for the equilibrium between the exciplex and the triplet state of RB in the 532-nm laser-photolyzed solution of ethylene glycol.

Conclusions

For the oxygen quenching of the excited triplet state of RB in EG, the bimolecular dissociation of the exciplex to products is important together with the unimolecular reaction. In particular, at high temperatures from 130 to 140 °C, the oxygen quenching of the triplet-state RB cannot be explained by kinetic Scheme 1 first postulated by Gijzeman et al.[10,11] but instead corresponds to kinetic Scheme 2 involving the bimolecular dissociation to products by oxygen in addition to a unimolecular process. The linear oxygen dependence of the quenching constant k_{obs} observed at room temperature reflects the attainment of the exciplex equilibrium even at low oxygen concentrations due to the large exothermic enthalpy of the exciplex reaction and the bimolecular dissociation of the exciplex by oxygen. The reaction enthalpy of the exciplex formation was estimated to be ca. 150 kJ mol^{-1}.

References and Notes

(1) Kahn, A. U. In *Singlet O_2*; Frimer, A. A., Ed.; CRC Press: Boca Raton, FL, 1985; Vol. I, pp 39−79.

(2) Richmond, R. C.; O'Hara, J. A. *Photochem. Photobiol.* **1993**, *57*, 291−297.

(3) Jori, G.; Brown, S. B. *Photochem. Photobiol. Sci.* **2004**, *3*, 403−405.

(4) Matsumoto, M. In *Singlet O_2*; Frimer, A. A., Ed.; CRC Press: Boca Raton, FL, 1985; Vol. I, pp 205−272.

(5) Foote, C. S.; Clennan, E. L. In *Active oxygen in chemistry*; Foote, C. S., Valentine, J. S., Greenberg, A., Liebman, J. F., Eds.; Blackie: London, 1995; pp 105−140.

(6) Dougherty, T. J.; Gormer, C. J.; Henderson, B. W.; Jori, G.; Kessel, D.; Korbelik, M.; Moan, J.; Peng, Q. *J. Natl. Cancer Inst.* **1998**, *80*, 889−902.

(7) Allen, C. M.; Sharman, W. M.; Van Lier, J. E. *J. Porphyrins Phthalocyanines* **2001**, *5*, 161−169.

(8) Kawaoka, K.; Khan, A. U.; Kearns, D. R. *J. Chem. Phys.* **1967**, *46*, 1842−1852.

(9) Birks, J. B. *Photophysics of Aromatic Molecules*; Wiley-Interscience: London, 1970, 492−517.

(10) Gijzeman, O. L. J.; Kaufman, F.; Porter, G. *J. Chem. Soc., Faraday Trans. 2* **1973**, *69*, 708−720.

(11) Gijzeman, O. L. J.; Kaufman, F. *J. Chem. Soc., Faraday Trans. 2* **1973**, *69*, 721−726.

(12) Rodgers, M. A. J.; Snowden, P. T. *J. Am. Chem. Soc.* **1982**, *104*, 5541−5543.

(13) Rodgers, M. A. J. *J. Am. Chem. Soc.* **1983**, *105*, 6201−6205.

(14) Schmidt, R.; Brauer, H.-D. *J. Am. Chem. Soc.* **1987**, *109*, 6976−6981.

(15) Scurlock, R. D.; Ogilby, P. R. *J. Phys. Chem.* **1987**, *91*, 4599−4602.

(16) Darmanyan, A. P. *Chem. Phys. Lett.* **1993**, *215*, 477−482.

(17) Scurlock, R. D.; Nonell, S.; Braslavsky, S. E..; Ogilby, P. R. *J. Phys. Chem.* **1995**, *99*, 3521−3526.

(18) Darmanyan, A. P. *J. Phys. Chem. A* **1998**, *102*, 9833−9837.

(19) Iu, K.-K.; Ogilby, P. R. *J. Phys. Chem.* **1987**, *91*, 1611−1617.

(20) Iu, K.-K.; Ogilby, P. R. *J. Phys. Chem.* **1988**, *92*, 4662−4666.

(21) Schmidt, R.; Afshari, E. *J. Phys. Chem.* **1990**, *94*, 4377−4378.

(22) Schmidt, R.; Tanielian, C.; Dunsbach, R.; Wolf, C. *J. Photochem. Photobiol., A* **1994**, *79*, 11−17.

(23) Scurlock, R. D.; Wang, B.; Ogilby, P. R. *J. Am. Chem. Soc.* **1996**, *118*, 388−392.

(24) Shimizu, O.; Watanabe, J.; Imakubo, K.; Naito, S. *Chem. Lett.* **1997**, 203−204.

(25) Shimizu, O.; Watanabe, J.; Imakubo, K.; Naito, S. *Chem. Lett.* **1999**, 67−68.

(26) Darmanyan, A. P.; Jenks, W. S.; Jardon, P. *J. Phys. Chem. A* **1998**, *102*, 7420−7426.

(27) Frederiksen, P. K.; Mcllroy, S. P.; Nielsen, C. B.; Nikolajsen, L.; Skovsen, E.; Jorgensen, M.; Mikkelsen, K. V.; Ogilby, P. R. *J. Am. Chem. Soc.* **2005**, *127*, 255−269.

(28) Murov, S. L.; Carmichael, I.; Hug, G. L. *Handbook of Photochemistry*; Mercel Dekker: New York, 1993.

(29) Cebul, F. A.; Kirk, K. A.; Lupo, D. W.; Pittenger, L. M.; Schuh, M. D.; Willams, I. R.; Winston, G. C. *J. Am. Chem. Soc.* **1980**, *102*, 5656−5661.

(30) Scurlock, R. D.; Ogilby, P. R. *J. Phys. Chem.* **1989**, *93*, 5493−5500.

(31) Kristiansen, M.; Scurlock, R. D.; Iu, K.-K.; Ogilby, P. R. *J. Phys. Chem.* **1991**, *95*, 5190−5197.

(32) McLean, A. J.; Rodgers, M. A. J. *J. Am. Chem. Soc.* **1992**, *114*, 3145−3147.

(33) McLean, A. J.; Rodgers, M. A. J. *J. Am. Chem. Soc.* **1993**, *115*, 4786−4792.

(34) McLean, A. J.; Rodgers, M. A. J. *J. Am. Chem. Soc.* **1993**, *115*, 9874−9875.

(35) Darmanyan, A. P.; Foote, C. S. *J. Phys. Chem.* **1992**, *96*, 3723−3728.

(36) McGarvey, D. J.; Szekeres, P. G.; Wilkinson, F. *Chem. Phys. Lett.* **1992**, *199*, 314−319.

(37) Darmanyan, A. P.; Foote, C. S. *J. Phys. Chem.* **1993**, *97*, 5032−5035.

(38) Grewer, C.; Brauer, H.-D. *J. Phys. Chem.* **1993**, *97*, 5001−5006.

(39) Smith, G. J. *J. Am. Chem. Soc.* **1994**, *116*, 5005−5006.

(40) Wilkinson, F.; McGarvey, D. J.; Olea, A. F. *J. Phys. Chem.* **1994**, *98*, 3762−3769.

(41) Wilkinson, F.; Abdel-Shafi, A. A. *J. Phys. Chem. A* **1997**, *101*, 5509−5516.

(42) Wilkinson, F.; Abdel-Shafi, A. A. *J. Phys. Chem. A* **1999**, *103*, 5425−5435.

(43) Abdel-Shafi, A. A.; Worral, D. R.; Wilkinson, F.; *J. Photochem. Photobiol., A* **2001**, *142*, 133−143.

(44) Mehrdad, Z.; Noll, A.; Grabner, E.-W.; Schmidt, R. *J. Phys. Chem. A* **2002**, *106*, 228−235.

(45) Mehrdad, Z.; Noll, A.; Grabner, E.-W.; Schmidt, R. *Photochem. Photobiol. Sci.* **2002**, *1*, 263−269.

(46) Schweitzer, C.; Mehrdad, Z.; Noll, A.; Grabner, E.-W.; Schmidt, R. *J. Phys. Chem. A* **2003**, *107*, 2192−2198.

(47) Wade, M. J.; Spikes, J. D. *Photochem. Photobiol.* **1971**, *28*, 221−224.

(48) Kochevar, I. E.; Lynch, M. C. *Photochem. Photobiol.* **2000**, *72*, 548−553.

(49) Douglas, P.; Waechter, G.; Mills, A. *Photochem. Photobiol.* **1990**, *52*, 473−479.

(50) Islam, S. D.-M.; Yoshikawa, Y.; Fujitsuka, M.; Watanabe, A.; Ito, O. *Bull. Chem. Soc. Jpn.* **1998**, *71*, 1543−1548.

(51) Neckers, D. C. *J. Photochem. Photobiol., A* **1989**, *47*, 1−29.

(52) Shimizu, O.; Watanabe, J.; Naito, S. *Chem. Phys. Lett.* **2000**, *332*, 295−298.

(53) Islam, S. D.-M.; Ito, O. *J. Photochem. Photobiol., A* **1999**, *123*, 53−59.